Acta Cryst. (1981). B**37**, 2019–2026

The Crystallization and Structure Determination of an Active Ternary Complex of Pig Heart Lactate Dehydrogenase

BY ULRICH M. GRAU AND MICHAEL G. ROSSMANN*

Department of Biological Sciences, Purdue University, West Lafayette, Indiana 47907, *USA*

AND WOLFGANG E. TROMMER

Institut für Organische Chemie, Biochemie und Isotopenforschung der Universität Stuttgart, Pfaffenwaldring 55, 7000 *Stuttgart* 80, *Federal Republic of Germany*

(*Received* 30 *July* 1980; *accepted* 6 *April* 1981)

Abstract

The ternary complex of pig heart H_4 lactate dehydrogenase with the enzymatically active covalent coenzyme substrate analog *S*-lac-NAD$^+$ crystallizes in space group $P3_221$ with three tetramers per unit cell and $a = 133{\cdot}6$, $c = 113{\cdot}5$ Å. The initial phases were determined from the known 3·0 Å resolution structure of a ternary complex with dogfish M_4 lactate dehydrogenase and then refined to 2·7 Å resolution by repeated cycles of molecular replacement, averaging over the two non-crystallographically related subunits. The final *R* factor was 0·196 including 22 588 observed reflections.

Introduction

Lactate dehydrogenase (LDH; EC 1.1.1.27) is a tetrameric enzyme of M_r 144 000. It catalyzes the last step of the glycolytic pathway in oxidizing lactate to pyruvate which, under anaerobic conditions, recycles NADH and thus ultimately leads to the production of the energy metabolite ATP. Several genetically distinct isoenzymes are known, the most common being M (designating the muscle type) and H (designating the heart type). Hybrids between these are found *in vivo* and *in vitro*.

The crystal structures of the homotetrameric dogfish M_4 LDH and several of its ternary inhibitor complexes have been determined to 2·0 and 3·0 Å resolution, respectively (Adams, Haas, Jeffery, McPherson, Mermall, Rossmann, Schevitz & Wonacott, 1969; Smiley, Koekoek, Adams & Rossmann, 1971; Chandrasekhar, McPherson, Adams & Rossmann, 1973; Adams, Buehner, Chandrasekhar, Ford, Hackert, Liljas, Rossmann, Smiley, Allison, Everse, Kaplan & Taylor, 1973; White, Hackert, Buehner, Adams, Ford, Lentz, Smiley, Steindel & Rossmann, 1976). The largest difference between the M_4 apoenzyme and the ternary complex structures is the conformation of the loop region (residues 99–113) which is folded down over the active site if the coenzyme and substrates are bound and provides in part the structural explanation for catalysis.

In order to study catalytic questions in more detail, the covalent substrate analog 3-*S*-[5-(3-carboxy-3-hydroxypropyl)]NAD$^+$ (*S*-lac-NAD$^+$) (Fig. 1) had been designed in accordance with the known structure of LDH. Here, the substrate *S*-lactate is covalently attached to the 5 position of the NAD$^+$ coenzyme. A methylene spacer was introduced to permit the substrate to bind in the same manner as the natural substrate. Indeed, it had been shown that LDH catalyzes an intramolecular redox reaction within *S*-lac-NAD$^+$ to produce the analog pyr-NADH (Grau, Kapmeyer & Trommer, 1978) and *vice versa* (Kapmeyer, Pfleiderer & Trommer, 1976). However, the rate of this reaction was decreased by a factor of approximately 2000 because the step-by-step dissociation of *S*-lactate and NAD$^+$ required in LDH has been made impossible by the covalent link. The covalent analog *S*-lac-NAD$^+$, therefore, offered the unique possibility to study an active ternary complex of LDH. We chose LDH from pig heart for this work because the kinetic analyses had been performed with this isoenzyme and to give some insight into isoenzyme differences.

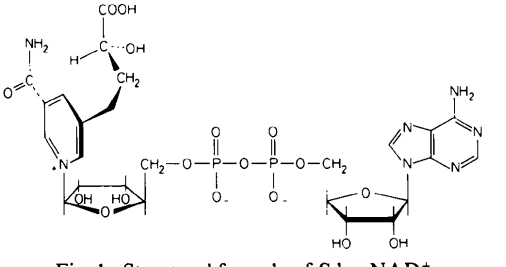

Fig. 1. Structural formula of *S*-lac-NAD$^+$.

* To whom reprint requests should be addressed.

0567-7408/81/112019-08$01.00

1. Materials

LDH was isolated from fresh pig hearts using affinity chromatography on immobilized oxamate in the presence of NADH as the essential purification step (Eventoff, Olsen & Hackert, 1974). After other LDH hybrid tetramers had been separated on a DEAE Sephadex A50 column the yield of the H_4 homotetramer was 267 mg from 460 g tissue. The isoenzyme purity was confirmed by slab gel electrophoresis.

It is known, however, that a small amount of NADH tightly binds to LDH which cannot be removed by extensive dialysis (Wieland, Duesberg, Pfleiderer, Stock & Sann, 1962). Furthermore, *S*-lac-NAD$^+$ exhibits poorer binding to LDH than NADH. Therefore, the removal of residual NADH seemed essential and was achieved by further purification over Sephadex G25 containing 5 mg ml^{-1} gel acid activated charcoal. Subsequent control experiments showed that pig H_4 LDH which had not been charcoal treated did not form crystals of the *S*-lac-NAD$^+$ ternary complex. The final, charcoal-treated pig H_4 LDH preparation exhibited a specific activity of 427×10^6 mol kg^{-1} s^{-1} (Bergmeyer, 1970) and $A_{280}/A_{260} = 3{\cdot}17$. The *S*-lac-NAD$^+$ was synthesized and analyzed for absolute purity as described earlier (Grau *et al.*, 1978). Sephadex gels were purchased from Pharmacia, Sweden. The charcoal used was Norit A from Serva, Heidelberg. All chemicals were of the highest purity grade available.

2. Crystallization of pig H_4 LDH/*S*-lac-NAD$^+$

Crystallization of the complex of pig H_4 LDH/*S*-lac-NAD$^+$ was achieved using the vapor-diffusion technique (*cf.* McPherson, 1976). Conditions after equilibration were: 34 mg ml^{-1} pig H_4 LDH, *S*-lac-NAD$^+$ 44 m*M* in *M*/50 sodium phosphate buffer pH = 7·6 containing 1·10 *M* sodium citrate. Large hexagonally shaped crystals (Fig. 2) grew within several days at room temperature to dimensions of about 0·5 mm thick and 1 mm long.

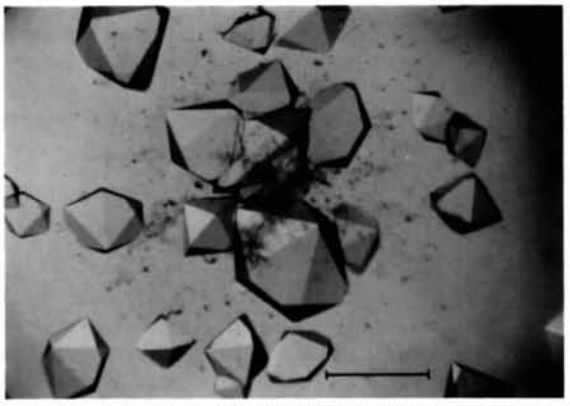

Fig. 2. Crystals of pig H_4 LDH/*S*-lac-NAD$^+$ as grown from sodium citrate. The bar corresponds to 1 mm.

Crystallization of pig H_4 LDH/*S*-lac-NAD$^+$ under conditions similar to those found for pig H_4 LDH/NADH/oxamate was unsuccessful. The latter had been crystallized using the batch method and ammonium sulfate as precipitant (Eventoff, Hackert & Rossmann, 1975). This fact was not due to the enzyme preparation since the pig H_4 LDH/NADH/oxamate crystals could be reproduced easily with both charcoal-treated pig H_4 LDH and untreated enzyme.

3. Space-group determination

The space group of pig H_4 LDH/*S*-lac-NAD$^+$ crystals was determined by taking 9° screened precession photographs of the principal zones. Cu $K\alpha$ radiation was produced by use of an Ni filter with a Cu target tube operated at 35 kV and 20 mA. The pattern along the morphological sixfold axis showed only threefold symmetry on *hk*1 photographs. Twofold symmetry was found along [*hhl*] and the 00*l* reflections were present at only every third reflection. These findings are consistent with space group $P3_221$ or $P3_121$. The unit-cell parameters are $a = 133{\cdot}6$ Å and $c = 113{\cdot}5$ Å. Subsequently it was shown that the correct hand for LDH corresponded to the $P3_221$ space group.

Packing considerations, without knowledge of molecular orientation or position, did not permit a differentiation between the possibilities of six or three molecules per unit cell, that is one or one-half molecule per asymmetric unit, respectively. The former would have represented an unusually tight packing as indicated by $V_M = 2{\cdot}02$ Å^3 dalton^{-1} whereas the latter would indicate an unusually loose packing ($V_M = 4{\cdot}03$ Å^3 dalton^{-1}) (Matthews, 1968).

4. High-resolution data collection and processing

Native high-resolution data were collected using oscillation photography (Arndt & Wonacott, 1977) on a Nonius camera attached to an Elliott GX6 rotating anode tube operated at 35 kV, 35 mA. The generator was equipped with a 200 μm focal cup and a copper target. The radiation was filtered with a nickel foil. Crystal-to-film distance was 75 mm. The crystals were mounted with their c^* axis along the spindle axis, permitting observation of almost a complete unique portion of reciprocal space within a 30° rotation. Each individual photograph was oscillated through 1·5° with 0·3° overlap on adjacent films. Exposure time was about 20 h. To record strong inner reflections as non-overloads, three films were stacked behind each other in a pack. A maximum of three data shots were taken from any one crystal. The total exposure time,

Table 1. *Summary of scaling of pig* H_4 LDH/*S*-lac-NAD^+ *data*

Number of cycles	Mode	R^* (%)	Cutoff	Remarks
5	Linear scale factors	10·9	2σ	
5	Anisotropic scale factors, φ_x, φ_y, a, b, post-refinement	10·6	2σ	$\Delta\varphi \sim 0{\cdot}005°$
5	Anisotropic scale factors, mosaic spread, post-refinement	10·2	2σ	Mosaic spread changed from 0·2 to 0·225°
3	Anisotropic scale factors	10·1	$1{\cdot}5\sigma$	46 366 total observed reflections 24 412 independent reflections

$$^*R = \frac{\sum_h \sum_i (F_{hi}^2 - F_h^2)}{\sum_h \sum_i F_h^2} \times 100$$

where F_h^2 is the mean intensity over the i observations of reflection h.

Table 2. *Overall R factors for partially and wholly recorded reflections before and after post-refinement*

R is defined as in Table 1.

Partiality	0 → 0·2	0·2 → 0·4	0·4 → 0·6	0·6 → 0·8	0·8 → 1·0	Whole
Before	202·2	106·5	60·1	37·8	28·4	11·0
After	73·4	41·7	30·1	22·9	19·6	10·5

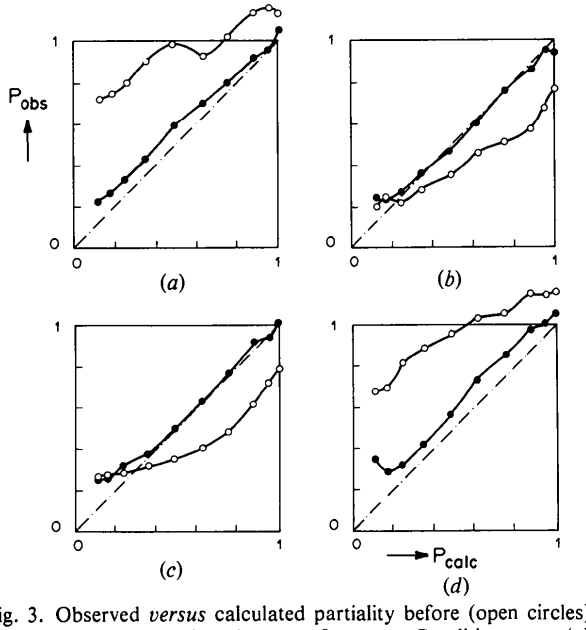

Fig. 3. Observed *versus* calculated partiality before (open circles) and after (closed circles) post-refinement. Conditions are (*a*) entering sphere, just penetrating; (*b*) entering sphere, almost within; (*c*) exiting sphere, just coming out; and (*d*) exiting sphere, almost out.

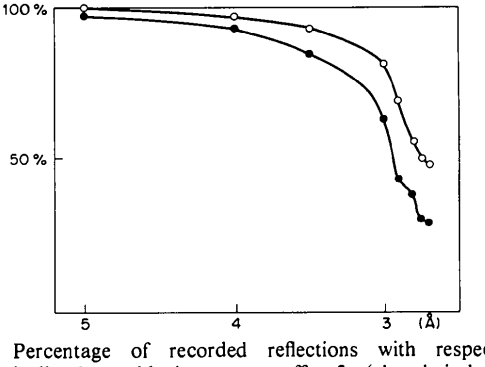

Fig. 4. Percentage of recorded reflections with respect to theoretically observable data at a cutoff at 2σ (closed circles) and $1{\cdot}5\sigma$ (open circles).

therefore, was well below 80 h, at which time the intensities started to show changes due to radiation damage.

The photographs were digitized on an Optronics P1000 scanner using a 100 μm raster step. The data were processed with the aid of an automatic convolution technique for refinement of crystal setting and final intensities were determined using variable profile fitting (Rossmann, 1979). Films within one pack were subsequently combined and scaled (Hamilton, Rollett & Sparks, 1965), resulting in an average $R = 9{\cdot}3\%$ (see Table 1 for definition of R). The film damping factor as determined from the refined scaling constants calculated to an average of 2·75 which is somewhat lower than expected for the film in use (Kodak Medical No-Screen). The mean intensity on the highest resolution range from 2·8 to 2·7 Å was around 1·4 standard errors in all films.

All films, covering 30°, were scaled together to yield the complete data set. A summary of the results is given in Table 1. After five cycles with linear scale factors, subsequent anisotropic scale factors converged quickly with $R = 10{\cdot}6\%$, which includes all reflections above two standard errors. Further improvement was reached in a procedure referred to as post-refinement (Rossmann, 1979), where the cell constants changed slightly from initially 133·5 to 133·6 Å and 112·7 to 113·5 Å for a and c, respectively. The crystal orientations changed by an average of only 0·005°, −0·028° being the largest adjustment. Mosaic-spread refinement posed some problems since it did not converge properly and the increasing values led to a concomitant loss of wholly recorded reflections, whereas it had little effect on the final R factors. Furthermore, the agreement between observed and calculated partiality, which should be linear, tended to become sigmoidal (Rossmann, Leslie, Abdel-Meguid & Tsukihara, 1979). A good compromise seemed to be reached at $m = 0{\cdot}225°$.

Post-refinement did improve the overall data quality considerably, very similar to the results on southern bean mosaic virus (SBMV) data collection (Rossmann *et al.*, 1979). This is shown in the analysis of partials (Fig. 3) and in the R factors (Table 2). For final scaling,

partials up to $p = 0{\cdot}6$ were used in the weighted average and the cutoff was chosen at $1{\cdot}5\sigma$. 46 366 useful reflections yielded a total of 24 412 unique reflections with $R = 10{\cdot}1\%$. About 50% of the theoretically observable data were recorded in the highest resolution range from 2·8 to 2·7 Å (Fig. 4). Many of them, however, are between 1·5 and 2·0 standard errors.

5. Molecular symmetry and orientation

A rotation function (Rossmann & Blow, 1962) was calculated to determine the orientation of the molecular twofold axes which relate the subunits in tetrameric LDH (Rossmann, Adams, Buehner, Ford, Hackert, Liljas, Rao, Banaszak, Hill, Tsernoglou & Webb, 1973). Data between 10 and 6 Å resolution were included and the Patterson origin was removed. For the inner summation, 268 large terms were selected, and the integration radius was 45 Å. Interpolation for the non-integral lattice points was over the 27 nearest reciprocal-lattice points. The coarse search was calculated in 5° intervals for ψ and φ with κ held constant at 180° [see Rossmann & Blow (1962) for definition of these spherical coordinates]. A number of peaks are present in the $a^* c^*$ as well as in the $a^* b^*$ planes. From these, two sets of orientations were plausible in that all three orthogonal molecular axes could be identified. A number of tests were performed to resolve this ambiguity by searching small angular intervals in the $b^* c^*$ plane by varying the integration radius, by altering the resolution cutoff and by improving the interpolation grid to a 5 × 5 × 5 size. When the function was computed with the better interpolation, a resolution range of 6 to 10 Å and a 45 Å integration radius, no doubt was left about the correct solution (Fig. 5). The molecular twofold axes were found to be oriented at $\psi = 90$, $\varphi = 35$, $\psi = 90$, $\varphi = 125°$ with the third axis running parallel to the crystallographic twofold axis along b.

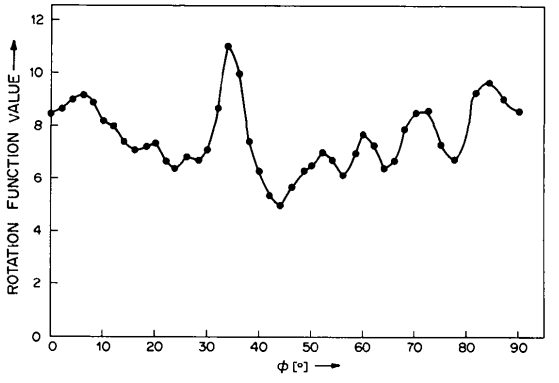

Fig. 5. Rotation function search for molecular twofold axes along the $a^* c^*$ plane. Conditions are given in the text.

The molecular axes relating the subunits in LDH have been labeled P, Q, and R (Rossmann *et al.*, 1973). To determine corresponding axes, a cross-rotation function was calculated. The density of one subunit of the previously determined structure of dogfish M_4 LDH/NADH/oxamate (White *et al.*, 1976) was cut out. Great care was taken to include all density belonging to the molecule by superimposing atomic positions on the density sections and determining the limits for each section accordingly. The tetramer was assembled with perfect 222 symmetry and with a known orientation of the P, Q and R axes. Structure factors were calculated for the tetramer density placed in a large ($a = b = c = 160$ Å) $P222$ cell (to avoid overlap of self-Pattersons) in this known orientation. Amplitudes between 5 and 10 Å were selected for the comparison rotation function. The Patterson origin was subtracted for the known structure. In this case, 296 large terms were selected and interpolation was over the 27 reciprocal-lattice points. The radius of integration was chosen as 55 Å. All possible combinations were calculated by pre-alignment of the molecular twofold axes, whose orientation had been determined by the self-rotation function with the P, Q and R axes of the known molecule. A search was then conducted by rotation about one of the superimposed axes in 5° intervals (Rossmann, Ford, Watson & Banaszak, 1972). The result is a single consistent

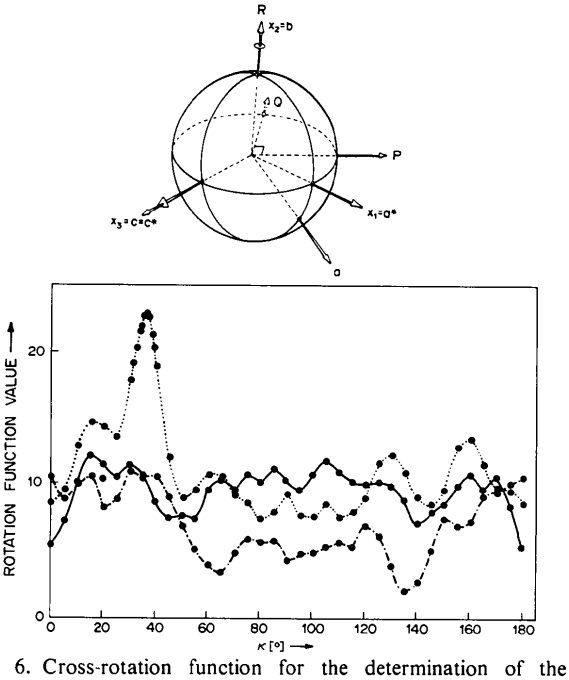

Fig. 6. Cross-rotation function for the determination of the molecular P, Q, and R axes in LDH. The molecular axis running along the crystallographic twofold axis in the pig H_4 LDH/S-lac-NAD^+ trigonal cell was pre-aligned with P (●——●), Q (●—·—·—●) and R (●·····●) of the known dogfish M_4 LDH/NADH/oxamate molecule followed by rotation about this axis. The resultant molecular orientation is depicted in the upper diagram. Conditions are detailed in the text.

solution, which is depicted in Fig. 6. Finally, a three-dimensional search in Eulerian space was conducted which verified the previous results. The molecular P axis in LDH/S-lac-NAD$^+$ crystals lies along $\psi = 90$, $\varphi = 35°$; the Q axis along $\psi = 90$, $\varphi = 125°$; and R along the crystallographic twofold axis in b.

6. Number of molecules per unit cell

The rotation function had shown that one molecular twofold axis (R) runs along the crystallographic twofold axis. In the rotation function, however, it cannot be distinguished whether these axes are coincident or merely parallel to each other. If they were parallel, a strong peak should be present in the Harker plane ($0vw$) of the Patterson map, corresponding to the vector $2\mathbf{y} + 2\mathbf{z}$. The Patterson map was calculated with data between 20 to 5 Å resolution and was completely flat except for the origin peak. Hence, the molecular R axis is found coincident with the crystallographic twofold axis ($u = v = 0$) which leaves three LDH tetramers in the unit cell.

7. Translation function

The pig H_4 LDH molecule occupies a special position in its trigonal cell and the translational problem is, therefore, reduced to a one-dimensional search along the twofold axis. Both enantiomorphous space groups $P3_221$ (a search along y at $z = \frac{1}{3}$) and $P3_121$ (a search along y at $z = \frac{1}{6}$) had to be considered.

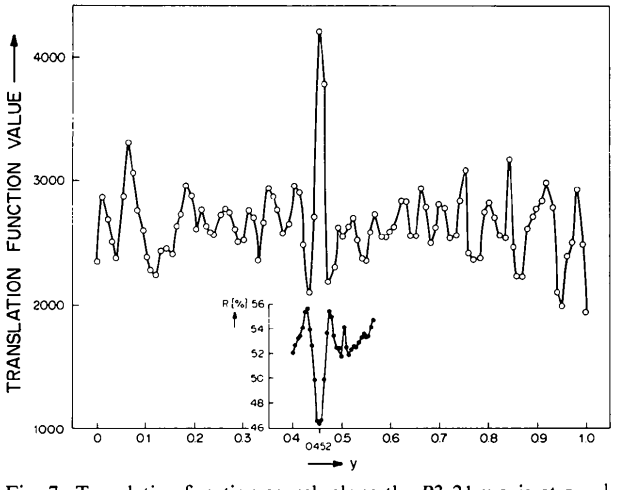

Fig. 7. Translation-function search along the $P3_221$ y axis at $z = \frac{1}{3}$ for determination of the molecular origin. The calculations performed with modified Fourier coefficients are shown on an arbitrary scale (open circles). Subsequent R-factor calculations (closed circles) yielded a position at $y = 0{\cdot}452$ for the origin of the pig H_4 LDH/S-lac-NAD$^+$ tetramer in its trigonal cell. $R = [(\sum ||F_{obs}| - k|F_{calc}||)/\sum |F_{obs}|] \times 100$.

The translation function (Rossmann & Blow, 1964; Argos & Rossmann, 1980) was calculated to set up 'Fourier' coefficients which allow a quick initial calculation. It computes the product $\sum_h F^2_{obs} F^2_{calc}$ for different positions of the known molecule in the unit cell. Hence a good correlation between F^2_{obs} and F^2_{calc} should produce a large peak. The F^2_{calc} values were derived from the known dogfish M_4 LDH/NADH/oxamate structure in the same large $P222$ unit cell. Data from 10 to 6 Å were used in the calculations. The molecules were properly pre-aligned according to the cross-rotation function results. The Fourier synthesis was calculated with a grid step of 1·34 Å along y. A sharp and large peak at $y = 0{\cdot}45$, $z = \frac{1}{3}$ was found (Fig. 7) with $P3_121$ symmetry.

Structure factors between 6 and 10 Å were then calculated for the known dogfish molecule in the proper orientation and positioned at $z = \frac{1}{3}$ in the $P3_221$ unit cell and y ranging from 0·4 to 0·56 in steps of 0·002 (corresponding to 0·27 Å). R factors between calculated and observed structure amplitudes were computed yielding a minimum of approximately 8% lower than background coincident with the translation-function peak position. The minimum is virtually symmetrical about $y = 0{\cdot}452$ and the half-width corresponds to about 2·5 Å (insert Fig. 7).

8. Crystal packing

The packing of the pig H_4 LDS/S-lac-NAD$^+$ molecules in the trigonal cell must be considered very loose indeed, given the volume V_M as 4·03 Å^3 dalton^{-1}. The only other ternary complexes of pig H_4 LDH crystallized so far have space group $C2$ with quite different molecular contacts. Presumably these differences must be attributed either to the crystallization conditions (sodium citrate in one case and ammonium sulfate in the other) or to the differences in molecular conformation of the complexed enzyme. It is noteworthy that it was not possible to crystallize pig H_4 LDH/S-lac-NAD$^+$ under the same conditions as pig H_4 LDH/NADH/oxamate (see above).

Not only are the contacts in the $C2$ cell different, but also the packing is much tighter, as indicated by $V_M = 2{\cdot}36$ Å^3 dalton^{-1}. In fact, all the LDH crystals analyzed so far showed much denser packing than the pig H_4 LDH/S-lac-NAD$^+$ complex (Table 3).

9. Molecular-replacement phase determination

Structure factors from 20 to 3 Å were calculated (using an adaptation of the translation-function program) for the ternary dogfish M_4 LDH molecule, oriented and placed properly in the $P3_221$ unit cell of pig H_4 LDH/S-lac-NAD$^+$. R factors between calculated and

Table 3. *Solvent content of* LDH *crystals*

Species	Complex	Space group	V_M (Å^3 dalton^{-1})	Reference
Dogfish M_4	Apo	$I422$	2·92	Adams *et al.* (1969)
Dogfish M_4	NAD^+ binary	$C4_22_12$	2·92	Adams *et al.* (1970)
Dogfish M_4	NAD-pyruvate	$C42_12$	2·70	Rossmann, Adams *et al.* (1972)
	NAD^+/oxalate			White *et al.* (1976)
	NADH/oxamate			White *et al.* (1976)
Mouse X_4	Apo	$P1$	2·70	Musick & Rossmann (1979)
Pig M_4	NAD-pyruvate	$P22_12_1$	2·51	Hackert *et al.* (1973)
	NADH/oxamate			Hackert *et al.* (1973)
Pig H_4	NAD^+/oxalate	$C2$	2·36	Eventoff *et al.* (1975)
	NADH/oxamate			Evantoff *et al.* (1975)
Pig H_4	*S*-lac-NAD^+	$P3_221$	4·03	

observed amplitudes are shown in Fig. 8 as a function of resolution. The overall R factor to 3 Å resolution was $R = 52{\cdot}2\%$, while to only 5 Å resolution it was 46%.

A 3·0 Å density map was calculated after combining the observed pig H_4 LDH/*S*-lac-NAD^+ amplitudes with the computed phases. The Fourier coefficients were weighted by Sim's coefficients (Sim, 1959, 1960).

10. Molecular-replacement averaging

Two identical subunits of the pig H_4 LDH/*S*-lac-NAD^+ tetramer form the asymmetric unit in the trigonal cell. The redundancy in information can be utilized to improve the phases by real-space averaging (Buehner, Ford, Moras, Olsen & Rossmann, 1974). A molecular envelope was first determined based on the dogfish M_4 LDH/NADH/oxamate atomic positions. This envelope was placed in the $P3_221$ unit cell in the proper orientation and position and the packing checked for possible overlap. Only minor modifications were necessary. Sorted data lists were then set up to relate non-crystallographically-related points within the envelope at every grid point in the $P3_221$ asymmetric unit. The corresponding density values were then supplied and averaged. The new density values are placed back into the trigonal cell asymmetric unit, expanded to the full cell and a back-transform calculated. The programs used in this study were those written by Johnson (1978), although similar programs have also been derived by Bricogne (1976). For averaging, the $P3_221$ cell was divided into 256 steps along x and y and 192 steps along z, which corresponds to a grid of approximately 0·5 Å spacing. The back-transform from 800 to 2·7 Å was calculated on an equally spaced grid. The Fourier programs used were those originally written by Ten Eyck (1973).

R factors, using a linear scale factor, were calculated for resolution shells of 2000 possible reflections each including those reflections beyond 3·0 Å which could not be phased before due to the resolution limit of the known structure. The R factors to 3·0 Å improved considerably whereas there is a steep increase between 3·0 and 2·7 Å resolution (Fig. 8). However, as the R factor was only 50% even in this range, it seemed reasonable to accept all these results for further phase refinement with molecular-replacement averaging in a single step. Moreover, since the size of F_{calc} in this resolution range was much smaller, Sim's weights showed a falloff at 3·0 Å, whereby the newly included reflections were down-weighted in the calculation of the next 2·7 Å resolution map.

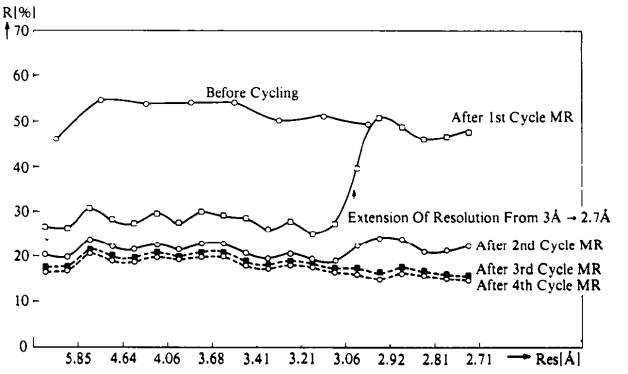

Fig. 8. R factors in resolution shells, each containing 2000 possible reflections, during molecular-replacement (MR) averaging iterations. Phases were extended from 3·0 to 2·7 Å resolution after cycle 1.

Three more cycles of molecular-replacement averaging were performed showing further improvement in the R factors, in particular for those high-resolution reflections which were included with extended molecular-replacement phases (Fig. 8). At this stage, convergence had apparently been reached as judged from lack of further improvement in the R factors, average phase shifts of less than 3°, and calculated Sim weights. The final overall R factor was 19·6% for the 22 588 reflections observed up to 2·7 Å resolution,

which compares favorably with the 18·9% for the 19 057 reflections within the initial resolution limit of 3·0 Å. The average phase shifts were 22·6° with respect to the initial molecular-replacement model. The shifts were distributed fairly uniformly over different resolution shells. An improvement of the map quality was obvious along with the improvement of R factors. The final map showed considerably more detail and a very low noise level as compared to either the first 3 Å molecular replacement map of pig H_4 LDH/*S*-lac-NAD^+ or the 3 Å map of dogfish M_4 LDH/NADH/oxamate.

The final electron density was displayed in an artificial orthogonal cell with the molecular P, $\bar{Q}$ and R axes along y, z and x, respectively. That is, skew sections were taken in the trigonal unit cell perpendicular to the molecular Q axis. Then sections were calculated in grid steps of 0·75 Å using the same programs as had been used for the averaging procedure described above. The electron density was drawn up for display in a Richards optical comparator (Richards, 1968) and a Watson–Kendrew model was fitted to the density using the known amino acid sequence of pig heart LDH (Eventoff, Rossmann, Taylor, Torff, Meyer, Keil & Kiltz, 1977). Atomic coordinates and structure factors have been deposited with the Brookhaven Protein Data Bank.*

11. Examination of possible bias from model phases

The final electron density map was inspected to determine whether or not the structure was biased due to the initial model phases. Residues where changes occur between the known pig H_4 (representing the current results) and dogfish M_4 (representing the initial phase model) LDH sequences (Eventoff *et al.*, 1977) can be used for this purpose. One such exchange occurs at position 42, where Met (dogfish) is replaced by Gly (pig). The pig H_4 LDH/*S*-lac-NAD^+ map, however, still shows a good piece of side-chain density for this residue. On the other hand, at positions 210*B* and 227, lysines are replaced by glutamines and in both cases the density indicates this exchange. Also, at position 231, where Asp is replaced by Met, the map shows the typical narrow, extended piece of density with its strongest part at the sulfur atom. In summary, the new sequence can be recognized in most positions but in some places there are some slight discrepancies.

The C-terminal helix was well defined in the dogfish M_4 LDH map. However, in the final pig H_4 LDH map, this part of the chain is weak and partially disordered. This disorder became more and more apparent as molecular replacement averaging proceeded.

The coenzyme density is a very prominent and well defined feature of the present map. Comparison to the corresponding density in the dogfish M_4 LDH map shows well defined differences. This is also true for the density of the substrate side chain in *S*-lac-NAD^+, which is located slightly differently from where the oxamate molecule was located, and shows features in accordance with the chemical differences. These differences will be discussed as part of a detailed analysis of the structure in a subsequent paper (Grau, Trommer & Rossmann, 1981).

We would like to thank Drs J. E. Johnson and M. R. N. Murthy for very beneficial discussions, in particular concerning the molecular-replacement averaging procedure. The interest of Dr W. D. L. Musick in this work was greatly appreciated. We would also like to thank Kathy Shuster for drawing some of the figures and Sharon Wilder for her knowledgeable assistance in the preparation of this manuscript. The work was supported by grants from the Deutsche Forschungsgemeinschaft to UMG and WET and by a National Institutes of Health grant (No. GM 10704) and a National Science Foundation grant (No. PCM78-16584) to MGR.

* Atomic coordinates and structure factors have been deposited with the Protein Data Bank, Brookhaven National Laboratory (Reference: 5LDH, R5LDHSF), and are available in machine-readable form from the Protein Data Bank at Brookhaven or one of the affiliated centers at Cambridge, Melbourne or Osaka. The data have also been deposited with the British Library Lending Division as Supplementary Publication No. SUP37000 (3 microfiche). Free copies may be obtained through The Executive Secretary, International Union of Crystallography, 5 Abbey Square, Chester CH1 2HU, England.

References

ADAMS, M. J., BUEHNER, M., CHANDRASEKHAR, K., FORD, G. C., HACKERT, M. L., LILJAS, A., ROSSMANN, M. G., SMILEY, I. E., ALLISON, W. S., EVERSE, J., KAPLAN, N. O. & TAYLOR, S. S. (1973). *Proc. Natl Acad. Sci. USA*, **70**, 1968–1972.

ADAMS, M. J., HAAS, D. J., JEFFERY, B. A., MCPHERSON, A. JR, MERMALL, H. L., ROSSMANN, M. G., SCHEVITZ, R. W. & WONACOTT, A. J. (1969). *J. Mol. Biol.* **41**, 159–188.

ADAMS, M. J., MCPHERSON, A. JR, ROSSMANN, M. G., SCHEVITZ, R. W. & WONACOTT, A. J. (1970). *J. Mol. Biol.* **51**, 31–38.

ARGOS, P. & ROSSMANN, M. G. (1980). *Theory and Practice of Direct Methods in Crystallography*, edited by M. F. C. LADD & R. A. PALMER, pp. 361–417. New York: Plenum Press.

ARNDT, U. W. & WONACOTT, A. J. (1977). *The Rotation Method in Crystallography*. Amsterdam: North-Holland.

BERGMEYER, H. U. (1970). *Methoden der Enzymatischen Analyse*, 2nd ed. Weinheim: Verlag Chemie.

BRICOGNE, G. (1976). *Acta Cryst.* A**32**, 832–847.

BUEHNER, M., FORD, G. C., MORAS, D., OLSEN, K. W. & ROSSMANN, M. G. (1974). *J. Mol. Biol.* **82**, 563–585.

CHANDRASEKHAR, K., MCPHERSON, A. JR, ADAMS, M. J. & ROSSMANN, M. G. (1973). *J. Mol. Biol.* **76**, 503–518.

EVENTOFF, W., HACKERT, M. L. & ROSSMANN, M. G. (1975). *J. Mol. Biol.* **98**, 249–258.

EVENTOFF, W., OLSEN, K. W. & HACKERT, M. L. (1974). *Biochim. Biophys. Acta*, **341**, 327–331.

EVENTOFF, W., ROSSMANN, M. G., TAYLOR, S. S., TORFF, H. J., MEYER, H., KEIL, W. & KILTZ, H. H. (1977). *Proc. Natl Acad. Sci. USA*, **74**, 2677–2681.

GRAU, U., KAPMEYER, H. & TROMMER, W. E. (1978). *Biochemistry*, **17**, 4621–4626.

GRAU, U. M., TROMMER, W. E. & ROSSMANN, M. G. (1981). *J. Mol. Biol.* In the press.

HACKERT, M. L., FORD, G. C. & ROSSMANN, M. G. (1973). *J. Mol. Biol.* **78**, 665–673.

HAMILTON, W. C., ROLLETT, J. S. & SPARKS, R. A. (1965). *Acta Cryst.* **18**, 129–130.

JOHNSON, J. E. (1978). *Acta Cryst.* A**34**, 576–577.

KAPMEYER, H., PFLEIDERER, G. & TROMMER, W. E. (1976). *Biochemistry*, **15**, 5024–5028.

MCPHERSON, A. JR (1976). *Methods of Biochemical Analysis*, edited by D. GLICK, Vol. 23, pp. 249–345. New York: John Wiley.

MATTHEWS, B. W. (1968). *J. Mol. Biol.* **33**, 491–497.

MUSICK, W. D. L. & ROSSMANN, M. G. (1979). *J. Biol. Chem.* **254**, 7611–7620.

RICHARDS, F. M. (1968). *J. Mol. Biol.* **37**, 225–230.

ROSSMANN, M. G. (1979). *J. Appl. Cryst.* **12**, 225–238.

ROSSMANN, M. G., ADAMS, M. J., BUEHNER, M., FORD, G. C., HACKERT, M. L., LENTZ, P. J. JR, MCPHERSON, A. JR, SCHEVITZ, R. W. & SMILEY, I. E. (1972). *Cold Spring Harbor Symp. Quant. Biol.* **36**, 179–191.

ROSSMANN, M. G., ADAMS, M. J., BUEHNER, M., FORD, G. C., HACKERT, M. L., LILJAS, A., RAO, S. T., BANASZAK, L. J., HILL, E., TSERNOGLOU, D. & WEBB, L. (1973). *J. Mol. Biol.* **76**, 533–537.

ROSSMANN, M. G. & BLOW, D. M. (1962). *Acta Cryst.* **15**, 24–31.

ROSSMANN, M. G. & BLOW, D. M. (1964). *Acta Cryst.* **17**, 1474–1475.

ROSSMANN, M. G., FORD, G. C., WATSON, H. C. & BANASZAK, L. J. (1972). *J. Mol. Biol.* **64**, 237–249.

ROSSMANN, M. G., LESLIE, A. G. W., ABDEL-MEGUID, S. S. & TSUKIHARA, T. (1979). *J. Appl. Cryst.* **12**, 570–581.

SIM, G. A. (1959). *Acta Cryst.* **12**, 813–815.

SIM, G. A. (1960). *Acta Cryst.* **13**, 511–512.

SMILEY, I. E., KOEKOEK, R., ADAMS, M. J. & ROSSMANN, M. G. (1971). *J. Mol. Biol.* **55**, 467–475.

TEN EYCK, L. F. (1973). *Acta Cryst.* A**29**, 183–191.

WHITE, J. L., HACKERT, M. L., BUEHNER, M., ADAMS, M. J., FORD, G. C., LENTZ, P. J. JR, SMILEY, I. E., STEINDEL, S. J. & ROSSMANN, M. G. (1976). *J. Mol. Biol.* **102**, 759–779.

WIELAND, T., DUESBERG, P., PFLEIDERER, G., STOCK, A. & SANN, E. (1962). *Arch. Biochem. Biophys. Suppl.* 1, pp. 260–263.

Acta Cryst. (1981). B**37**, 2026–2029

The Fundamental Structure of Cycasin, (Methyl-*ONN*-azoxy)methyl β-D-Glucopyranoside

BY M. KAWAMINAMI AND I. KAWANO

College of Liberal Arts, Kagoshima University, Korimoto, Kagoshima 890, *Japan*

A. KOBAYASHI, K. TADERA AND F. YAGI

Faculty of Agriculture, Kagoshima University, Korimoto, Kagoshima 890, *Japan*

AND S. KAWANO

College of General Education, Kyushu University, Ropponmatsu, Chuoku, Fukuoka 810, *Japan*

(*Received* 15 *December* 1980; *accepted* 3 *April* 1981)

Abstract

$C_8H_{16}N_2O_7$ is monoclinic, space group $C2$, with $a = 15{\cdot}422$ (1), $b = 4{\cdot}854$ (1), $c = 15{\cdot}754$ (1) Å, $\beta = 109{\cdot}83$ (1)°, $Z = 4$, $V = 1109{\cdot}4$ (5) Å^3, $M_r = 252{\cdot}22$, $D_m = 1{\cdot}49$, $D_x = 1{\cdot}51$ Mg m^{-3}. The structure was solved by the direct method using three-dimensional X-ray data and refined by the least-squares method to a final $R = 0{\cdot}100$ for 849 observed reflexions. In the crystal, a glucosyl part linked to the neighbouring glucosyl moieties by four different hydrogen bonds forms a double layer parallel to the (001) plane, and the aglycone parts are stretched in a direction perpendicular to the layers and have van der Waals contacts with other molecules.

Introduction

The compound cycasin was isolated as the toxic principle of the Japanese cycad, *Cycas revoluta* Thunb., and its chemical structure was determined as meth-

0567-7408/81/112026-04$01.00